Supporting Information

From Pair to Single: Sole Fluorophore for Ratiometric Sensing by Dual-Emitting Quantum Dots

College of Chemistry and Materials Science, Anhui Normal University, Wuhu, 241000, China.

Linlin Lu, Guang Yang and Yunsheng Xia*

E-mail address: xiayuns@mail.ahnu.edu.cn

1. Experimental Section

1.1 Characterizations

The photoluminescence (PL) and the absorption spectra were recorded with a Hitachi F-4600 fluorescence spectrophotometer and a Hitachi-U-3100 spectrophotometer, respectively. PL lifetime measurements were performed with the time correlated single photo counting technique on the combined steady state and lifetime spectrometer (Edinburgh Analytical Instruments, FLS920). The resonance light scattering spectra were obtained by synchronously scanning the excitation and emission monochromators ($\Delta\lambda$ = 0 nm) at F-4600 spectrophotometer. Characterizations of transmission electron microscopy (TEM) were carried out on Tecnai G2 20 ST (FEI) under the accelerating voltage of 200 kV. The samples for TEM measurements were prepared by the deposition of one drop of aqueous dispersion on a copper grid coated with thin films of carbon, and the solvent was removed by evaporation in air. The solutions were analyzed for ξ-potential values using dynamic light scattering (DLS, Zetasizer Nano ZS series, Malvern Instruments) with a 633 nm laser wavelength and a measurement angle of 173º (backscatter detection) at 25 °C. X-ray photoelectron spectroscopy (XPS) measurements were performed by an ESCALAB 250 Xi XPS system of Thermo Scientific, where the analysis chamber was 1.5×10^{-9} mbar, and the X-ray spot was 500mm. Quantitative High performance liquid chromatography (HPLC) was performed on a gradient high pressure liquid chromatograph (Shimadzu HPLC Class 10Aseries) with two LC-10AT pumps, a fixed wavelength programmable UV/VIS detector (SPD-10A), a guard column (ShimadzuTM, ODS 2 cm, Shim-pack) and RPC-18 column (150 mm × 4.6 mm i.d., particle size 5 μ) was used. Nuclear magnetic resonance (NMR) spectra were measured with a Bruker 400 Hz spectrometer. All pH values were measured with a model pHs-3c meter. The PL spectra were measured at room temperature, and the excitation wavelength was 300 nm. To avoid the interference of frequency doubling scattering, optical filter was used (at emission window) to remove the light below 350 nm.

1.2 Materials

3-mercaptopropionic acid (MPA, 97%) was purchased from Alfa Aesar. Cysteamine was purchased from Aladdin. 2-(Bromomethyl) phenylboronic acid and 4,4'-Dipyridyl were obtained from J&K Scientific (Shanghai, China). $ZnSO_4\cdot7H_2O$, $Mn(CH_3COO)_2\cdot4H_2O$, $Na_2S\cdot9H_2O$ were

purchased from Sigma-Aldrich. $HAuCl_4 \cdot 3H_2O$, $NaBH_4$ and other reagents used were acquired from Shanghai Reagent Co. All solutions were prepared with double deionized water.

1.3 Synthesis

1.3.1 Synthesis of N, N'-4, 4'-bis (benzyl-2-boronic acid) bi-pyridinium dibromide (BBV)

BBV was synthesized according to a literature method.[1] In brief, 0.87g (4.1 mmol) of 2-bromomethylphenylboronic acid in 7.5 mL DMF was added with 0.25 g (1.6 mmol) 4,4'-bipyridyl, the reaction was stirred for 48h at 70 °C under nitrogen. Then the mixture was cooled to room temperature, and the yellow precipitate was collected by centrifugation, washed with DMF, acetone and then diethyl ether and dried under a stream of nitrogen to yield BBV. The data of ^1H NMR (D_2O, 400MHz) is as follows, ^1H NMR: δ 9.01 (d, J = 7.2, 4H), 8.42 (d, J = 7.2 Hz, 4H), 7.75 (d, J = 6.6Hz 2H), 7.57 (m, 4H), 6.04 (s, 4H) (Figure S1.), and the high-performance liquid chromatography (HPLC) shows a high purity of BBV (99.5264%) (Figure S1.).

1.3.2 Synthesis and purification of the doped ZnS:Mn^{2+} QDs

MPA-capped doped ZnS:Mn^{2+} QDs were prepared aqueous solution using a modified method described previously.[2] Briefly, 7.5 mL of 0.1 M $ZnSO_4 \cdot 7H_2O$ and 100 μL of 0.1M $Mn(CH_3COO)_2$ were dissolved in 50 mL of water, and 2×10^{-3} mol of MPA was added under stirring. The mixed solution was adjusted to pH 10 with 1 M NaOH and stirred under nitrogen at room temperature for 30 min. Then, 7.5 mL of 0.1 M $Na_2S \cdot 9H_2O$ was injected to the above solution. The mixture was stirred for 10 min, and then the solution was aged at 50 °C under air for 5 h to form MPA capped Mn-doped ZnS QDs.

The obtained QDs were precipitated with ethanol, separated by centrifuging, washed with ethanol, and dried in a vacuum. The prepared QDs powder is highly water soluble.

1.3.3 Synthesis of positively charged gold nanoparticles (AuNPs)

Amine terminated AuNPs were prepared according to the reported literature.[3] Specifically, 400 μL of 213 mM cysteamine solution was added to 40 mL of 1.42 mM $HAuCl_4$ solution. The mixture was stirring for 20 min at room temperature in the dark. Then, 10 μL of 10 mM $NaBH_4$ solution was added, and the mixture was further stirred for 60 min in the dark.

1.4 Electron transfer system

1.4.1 Interaction of BBV and the QDs

200 μL of 0.1 M PBS buffer solution (pH = 7.4), 20 μL of the purified MPA-capped ZnS:Mn^{2+} QDs and a certain volume of BBV (3.42×10^{-6} M) were placed in a series of 5 mL colorimetric tubes. The mixtures were diluted to 3 mL with water and mixed thoroughly. 5 min later, their PL spectra were recorded with an excitation wavelength of 300 nm.

1.4.2 Interaction of QDs-BBV complex and glucose

200 μL of 0.1 M PBS buffer solution (pH = 7.4), 20 μL of the purified MPA-capped ZnS:Mn^{2+} QDs and 25 μL 3.42×10^{-5} M BBV were placed in a series of 5 mL colorimetric tubes. Then different amounts of glucoses were added. The mixtures were diluted to 3 mL with water and mixed thoroughly. 5 min later, their PL spectra were recorded with an excitation wavelength of 300 nm.

1.5 Energy transfer system

200 μL of 0.1 M Tris-HCl buffer solution (pH = 6.0), 20 μL of the purified MPA-capped ZnS:Mn^{2+} QDs and different amounts of AuNPs (from 0 to 0.256 nM) were added. The mixtures were diluted to 3 mL with water and mixed thoroughly. 5 min later, their PL spectra were recorded with an excitation wavelength of 300 nm.

1.6 Chemical reaction system

1.6.1 Interaction of the doped QDs and H_2O_2

200 μL of 0.1 M Tris-HCl buffer solution (pH = 7.0), 20 μL of the purified MPA-capped ZnS:Mn^{2+} QDs and different amounts of H_2O_2 (from 0 to 8.33 mM) were added. The mixtures were diluted to 3 mL with water and mixed thoroughly. 5 mins later, their PL spectra were recorded with an excitation wavelength of 300 nm.

1.6.2 Interaction of the doped QDs-H_2O_2 complex and SO_3^{2-}

200 μL of 0.1 M Tris-HCl buffer solution (pH = 7.0), 20 μL of the purified MPA-capped ZnS:Mn^{2+} QDs and 8.33 mM H_2O_2 were placed in a series of 5 mL colorimetric tubes. Then different amounts of SO_3^{2-} were added. The mixtures were diluted to 3 mL with water and mixed thoroughly. 5 min later, their PL spectra were recorded with an excitation wavelength of 300 nm.

1.7 PL properties of the doped ZnS:Mn^{2+} QDs at different experimental conditions

1.7.1 pH value

20 μL of the purified MPA-capped ZnS:Mn^{2+} QDs and 200 μL of different pH values PBS buffer

solution (From 5.0 to 8.9) were placed in a series of 5 mL colorimetric tubes. The mixtures were diluted to 3 mL with water and mixed thoroughly. 5 min later, their PL spectra were recorded with an excitation wavelength of 300 nm.

1.7.2 Excitation wavelength

20 μL of the purified MPA-capped ZnS:Mn^{2+} QDs and 200 μL of 0.1 M PBS buffer solution (pH = 7.4) were placed in a series of 5 mL colorimetric tubes. The mixtures were diluted to 3 mL with water and mixed thoroughly. 5 min later, their PL spectra were recorded with different excitation wavelength (from 240 nm to 320 nm).

1.7.3 Concentration effects

200 μL of 0.1 M PBS buffer solution (pH = 7.4) and different concentration of the ZnS:Mn^{2+} QDs were placed in a series of 5 mL colorimetric tubes. The mixtures were diluted to 3 mL with water and mixed thoroughly. 5 min later, their PL spectra were recorded with an excitation wavelength of 300 nm.

2. Quantum yield (QY) of the doped ZnS:Mn^{2+} QDs

The QY of the ZnS:Mn^{2+} QDs was measured according to the method described in Ref. 4.[4] Briefly, Rhodamine 6G (ethanol as solvent) was chosen as a reference standard (QY = 95%), the absorbance for the standard and the ZnS:Mn^{2+} colloid samples at the excitation wavelengths and the PL spectra of the same solutions were measured, respectively. The integrated PL intensity (that is, the area of the PL spectrum) from the fully corrected PL spectrum was calculated. Six respective different concentration solutions of Rhodamine 6G and ZnS:Mn^{2+} QDs (absorbance at excitation wavelength < 0.1) were used in the measurements. The areas of integrated PL intensity vs. absorbance were plotted. The plot obtained should be a straight line with a gradient M, which was used to calculate the QY according to the following Eq. (1):

$$\Phi_x = \Phi_s \left(\frac{M_x}{M_s} \right) \left(\frac{\eta_x}{\eta_s} \right)^2$$

Where the subscript s and χ denote standard and test samples, respectively. Φ is QY, and η is the refractive index of the solvent (ethanol: 1.36, water: 1.33). It should be noted that the excitation wavelength for measurements of QY was set at the excitonic absorption peak of the ZnS:Mn^{2+} QDs samples in the experiments.

According to above, the relative PL QY is estimated to be 15% for the doped ZnS:Mn^{2+} QDs.

3. Additional data

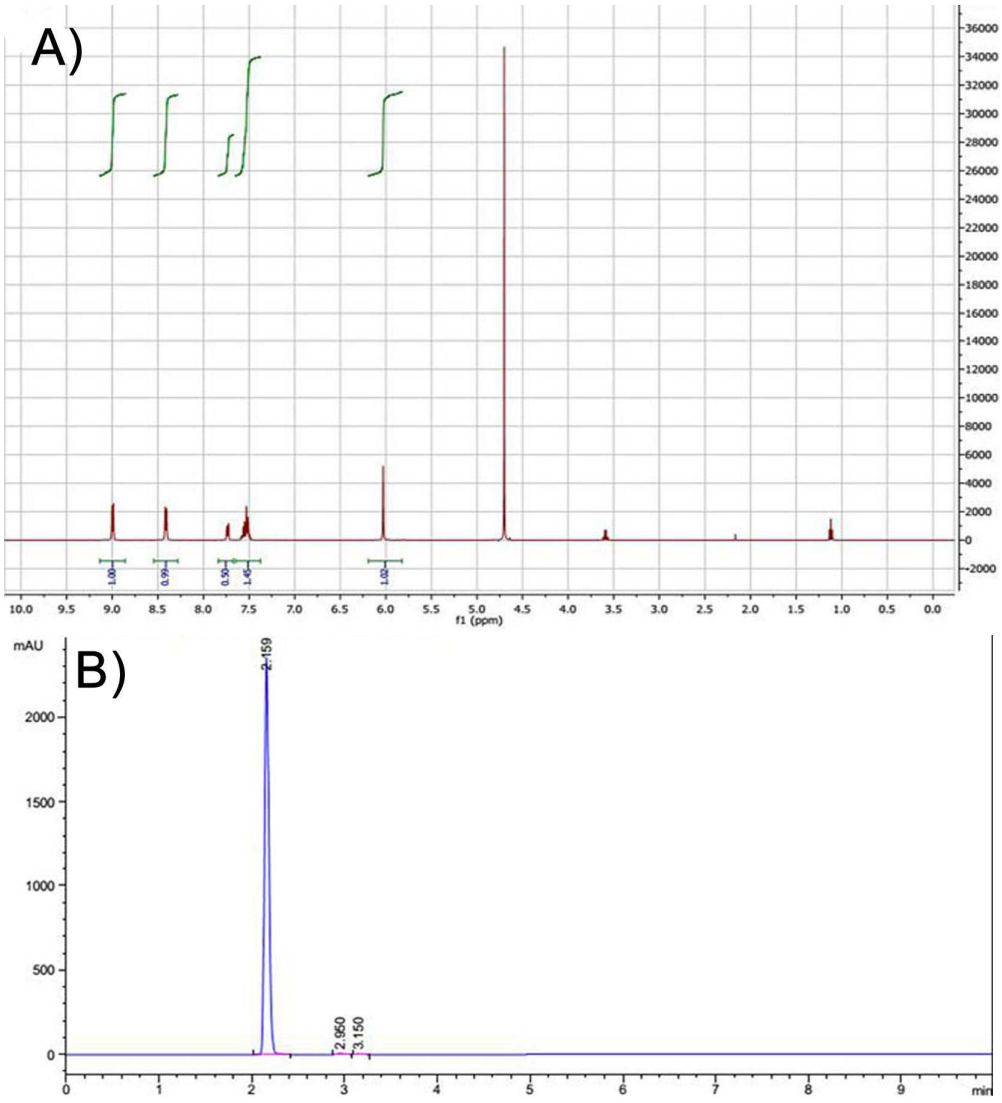

Figure S1. ^{1}H NMR spectrum (A) and HPLC chromatogram (B) of BBV (t_R = 2.159).

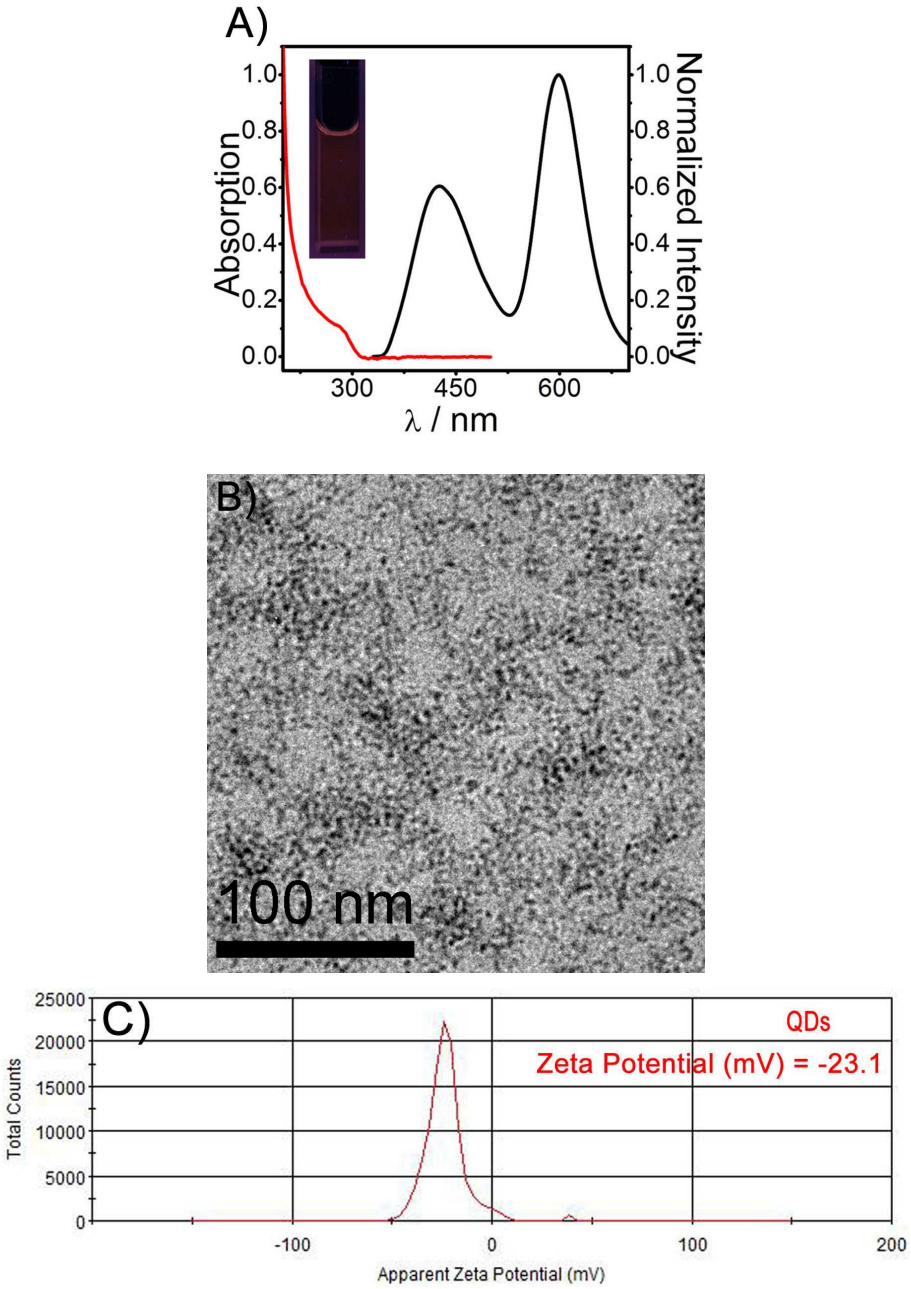

Figure S2. Characterizations of the doped ZnS:Mn^{2+} QDs. (A) Absorption (red line) and PL (black line) spectra. Inset: the photograph of the QD solution under UV (302 nm) light. (B) TEM image, the average size of the particles is about 4 nm. (C) ξ-potential value of the carboxyl terminated doped QDs.

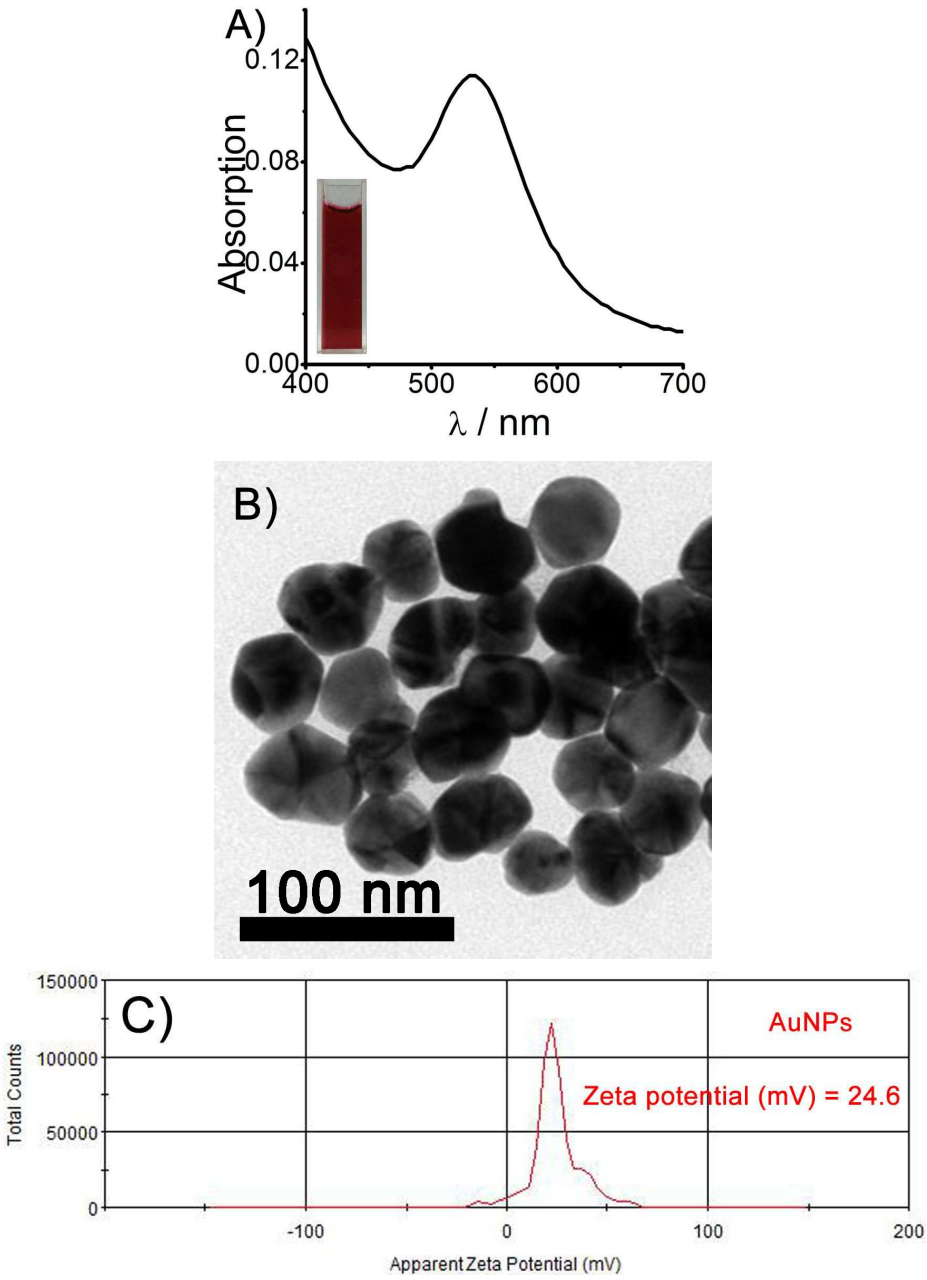

Figure S3. Characterization of the amine terminated AuNPs: (A) Absorption spectrum of the AuNPs. Inset: the photograph of the AuNPs under room light. (B) TEM image of the AuNPs. (C) ξ-potential value of the amine terminated AuNPs.

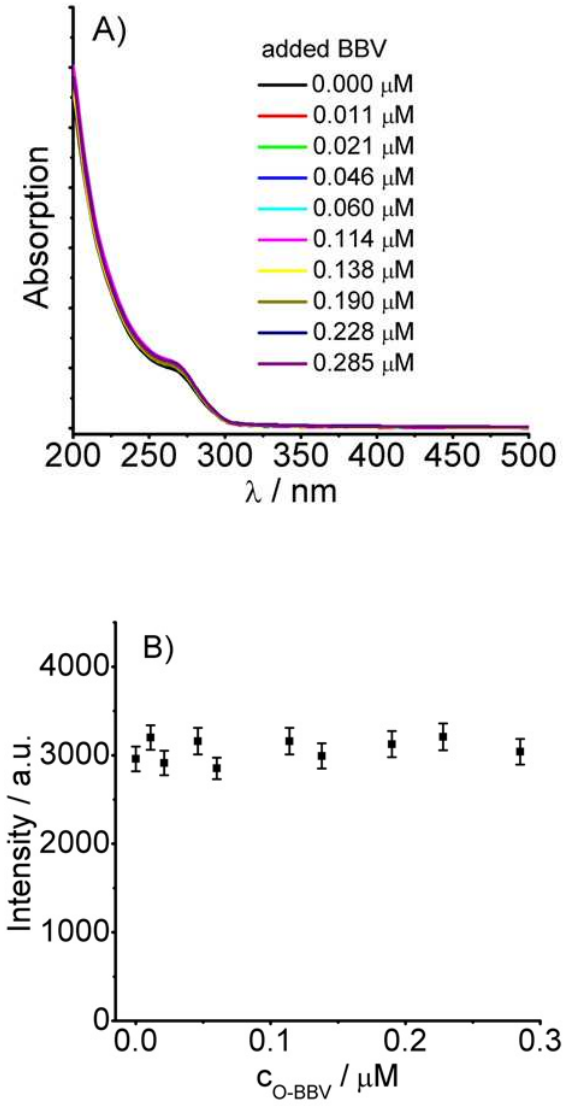

Figure S4. (A) Absorption spectra (A) and resonance light scattering intensities (B) of the doped QDs in the presence of various concentrations of BBV molecules. The almost invariable absorption edge (A) and resonance light scattering intensities (B) indicate that the QDs are well dispersed instead of aggregation together in the presence of BBV molecules.

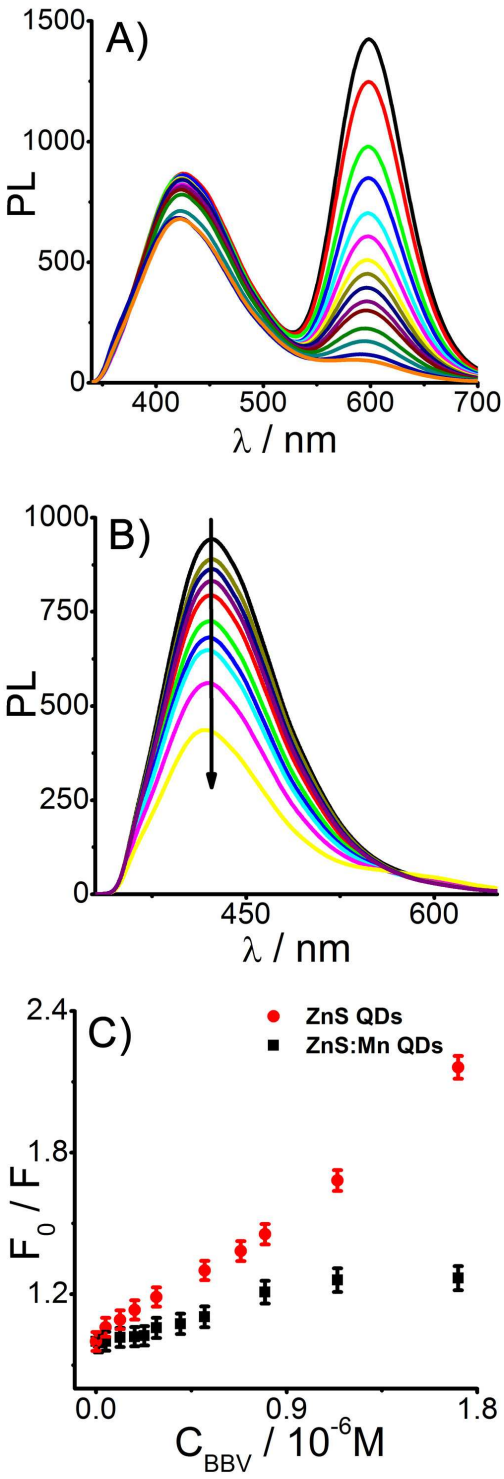

Figure S5. (A) PL spectra of the ZnS:Mn^{2+} QDs with increasing BBV (From 0 to 1.71 μM). (B) PL spectra of undoped ZnS QDs with increasing BBV (From 0 to 1.71 μM). (C) Plots of F_0/F vs. BBV concentration. F_0 and F are the PL intensities of the host emission of the QDs in the absence and presence of BBV, respectively.

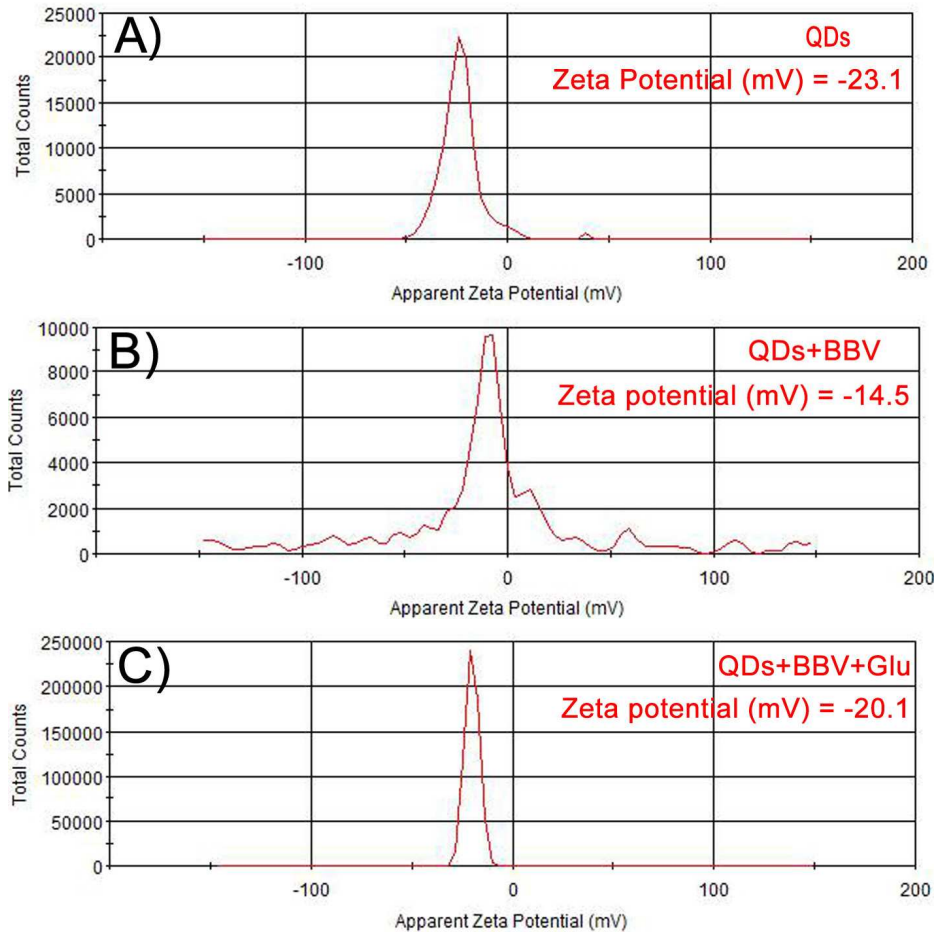

Figure S6. ξ-potential values of the doped ZnS:Mn^{2+} QDs (A), QDs + BBV (B), QDs + BBV + Glucose (C). The concentrations of the added BBV and glucose are 0.285 μM and 220 mM, respectively. To avoid the potential influence of pH, PBS buffer solutions (pH 7.4) were used for all the measurements.

As BBV molecules are added in the QD solution, the ξ-potential value changes from -23.1 mV to -14.5 mV. The decrease of surface charge is due to the fact that positively charged BBV and carboxyl groups at the ZnS:Mn^{2+} QD surface can bind each other and form a hybrid complex through electrostatic attraction. As glucose is added, the QD-BBV complex is broken because of the strong interaction of boronic acids with glucose, which leads to the recovery of ξ-potential value.

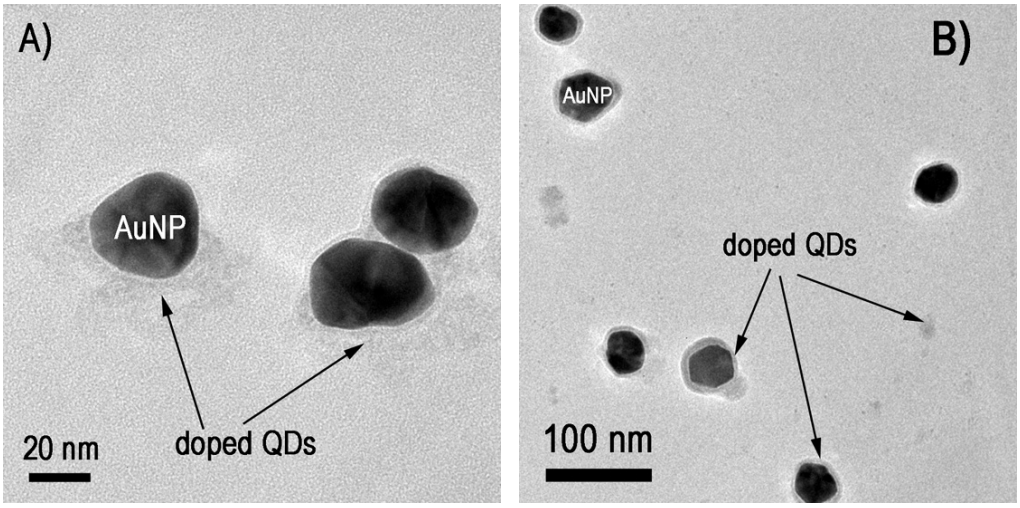

Figure S7. TEM images of the hybrid AuNP-QDs assemblies. Figure A shows the representative hybrid morphology of the AuNP-QDs assemblies, as the positively charged AuNPs and the negatively doped QDs interact with each other. Occasionally, more well-defined core/shell AuNP/QDs structure can also be observed (Figure B). We consider that the products shown in Figure A are more close to the assembly state in bulk solution, because the electrostatic attraction is not very strong. In terms of the formation of the well-defined core/shell structure (Figure B), additional reorganization processes may occur during dry on grid.

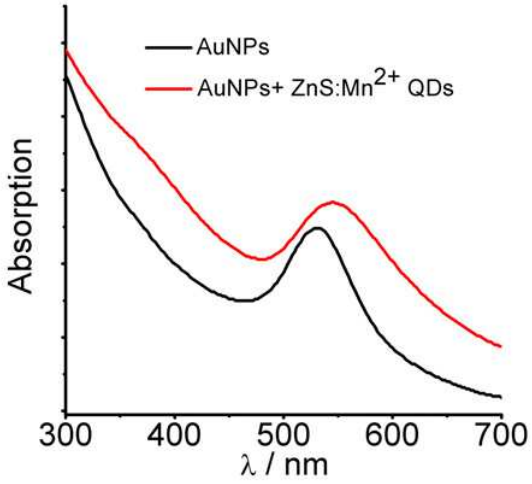

Figure S8. Representative absorption spectra of the amine terminated AuNPs in the absence and presence of the doped QDs. As the doped QDs are added to the AuNPs, the intensity of the AuNP SPR increases with an obvious bathochromic shift of the surface plasmon peak. This in-situ characterization demonstrates that (1) the AuNPs and the doped QDs formed hybrid assembly (core/shell structure) indeed; (2) the NPs do not aggregate each other. The reasons are as follows: First, the red shift of the surface plasmon peak results from that the AuNPs are surrounded by the doped QDs, because the refractive index of ZnS (n=2.57) is much larger than that of water (n=1.33).[5] Second, if AuNPs aggregate, the SPR intensity in 520 nm would decrease, and a new and broad absorption band would occur at 650-700 nm. The concentrations of the AuNPs and the doped QDs are 256 pM and 22 nM, respectively.

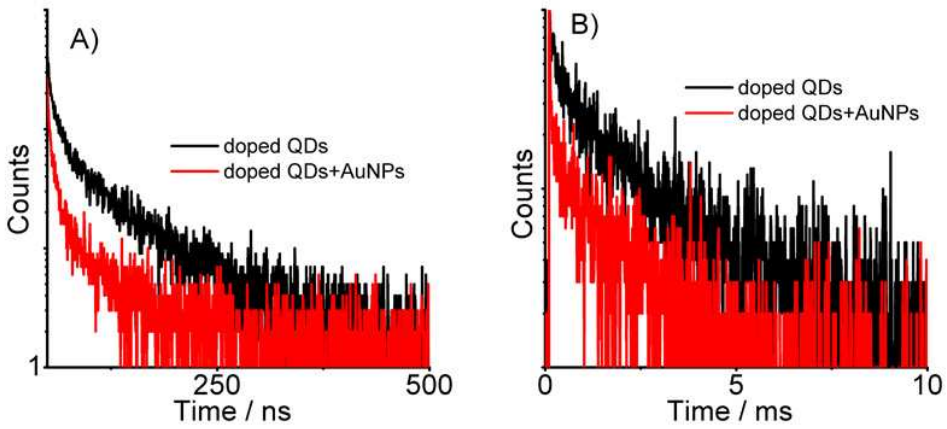

Figure S9. PL Lifetimes of the host (A) and Mn^{2+} (B) emission in the absence and presence of AuNPs. As the two particles form assembly, the decrease of decay time, both for the host and the Mn^{2+} emission, is observed, because of the additional decay channels provided by the AuNPs (energy acceptor).[6] The concentrations of the AuNPs and the doped QDs are 32 pM, and 22 nM, respectively.

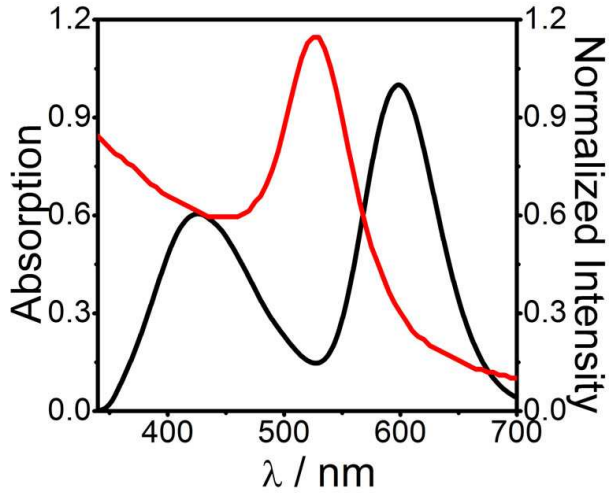

Figure S10. Normalized SPR absorption spectrum of the AuNPs and emission spectrum of the ZnS:Mn^{2+} QDs.

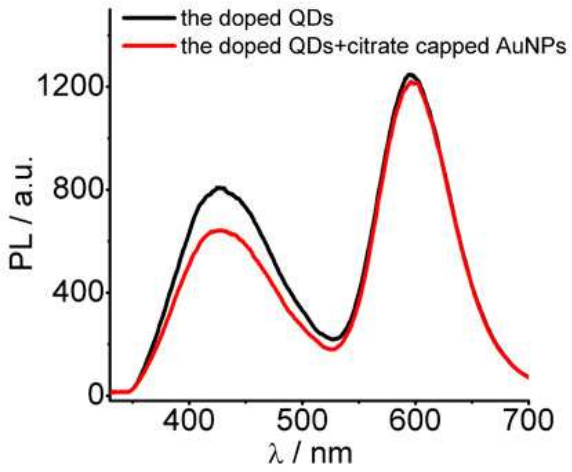

Figure S11. PL spectra of the doped QDs in the absence and presence of citrate capped AuNPs. Because both the two particles are negatively charged, they are well dispersed in solution by electrostatic repulsion. In the meantime, a small emission quenching (<20%) of the host emission is observed, which results from the scattering and/or self-absorption effects of the AuNPs. In contrast, the Mn^{2+} emission keeps rather well because of its longer emission wavelength (As we know, the longer wavelength, the weaker scattering effect). This quenching effect is a fixed value for a specific AuNP contained system, which does not impact the ratiometric sensing applications. The concentrations of the citrate capped AuNPs and the doped QDs are 256 pM, and 22 nM, respectively.

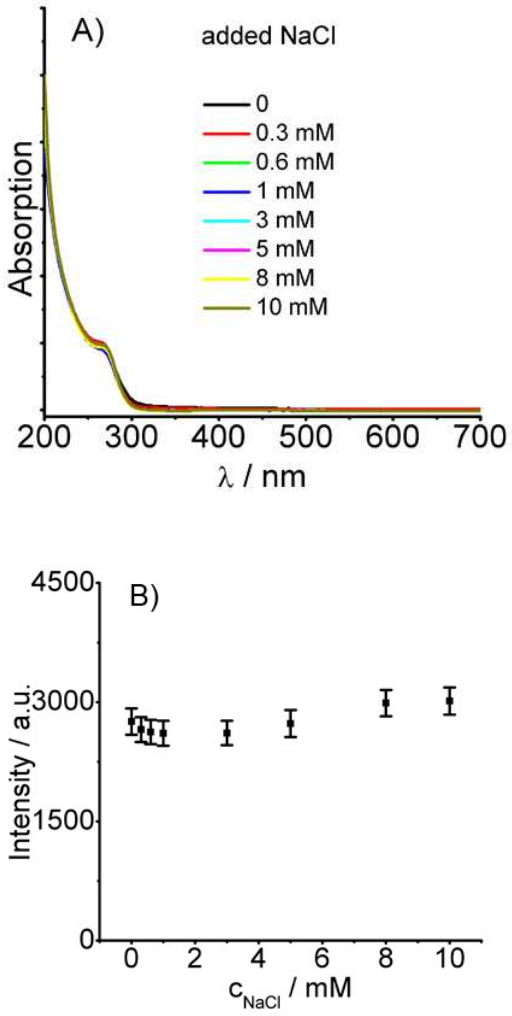

Figure S12. Absorption spectra (A) and resonance light scattering intensities (B) of the doped QDs in the presence of various concentrations of NaCl. The almost invariable absorption edge (A) and resonance light scattering intensities (B) indicate that the QDs are well dispersed instead of aggregation together in the presence of NaCl.

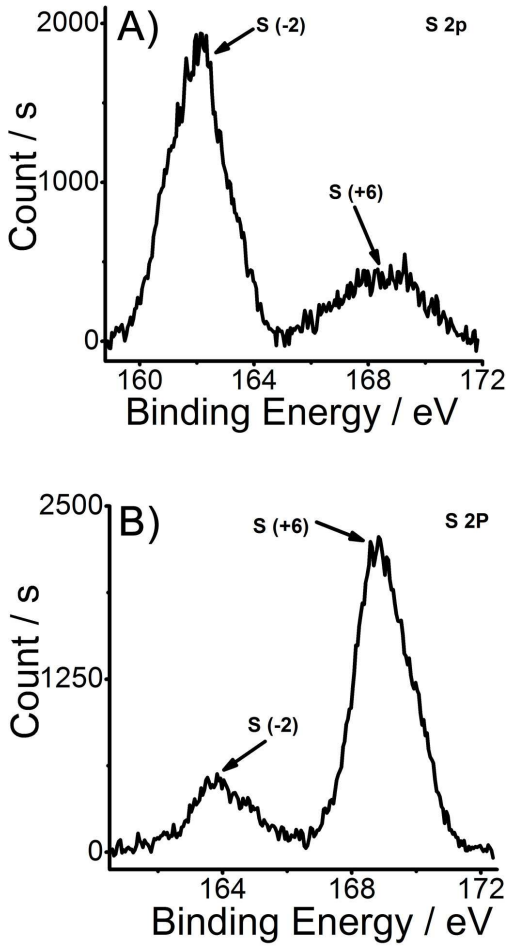

Figure S13. XPS patterns of S 2p peaks in ZnS:Mn^{2+} QDs before (A) and after (B) interaction with H_2O_2. For better observation, a little more H_2O_2 (14 mM) is added.

After interaction with H_2O_2, the ratio of S^{2-}/S^{6+} changes from 3.02 to 0.27, which indicates that the oxidation effect of H_2O_2. The pre-existed S^{6+} might be the oxidation effect of dissolved oxygen.

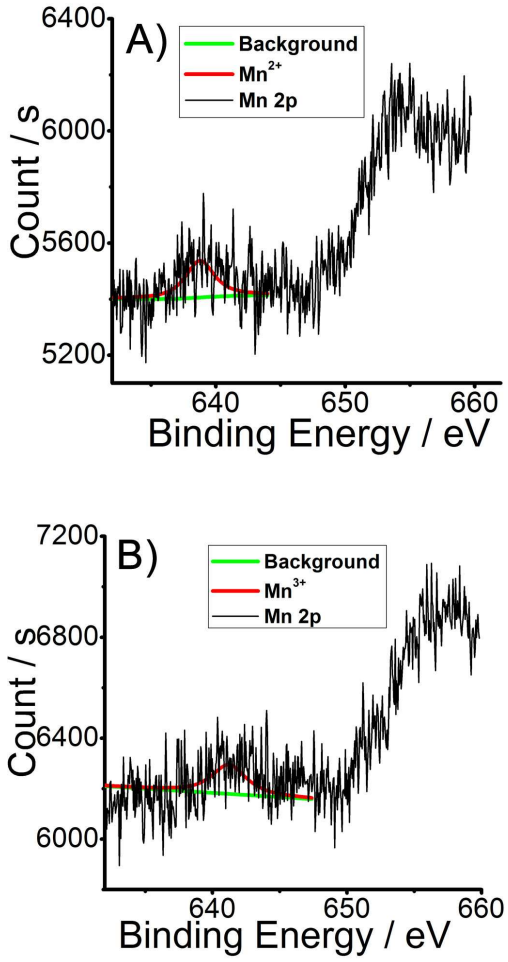

Figure S14. XPS patterns of Mn 2p peaks in the ZnS:Mn^{2+} QDs before (A) and after (B) interaction with H_2O_2. For better observation, a little more H_2O_2 (14 mM) is added. Despite high noise due to the low content, it is rather clear that a few Mn^{2+} ions (638 eV) are oxidized to Mn^{3+} ions (641 eV) by H_2O_2.

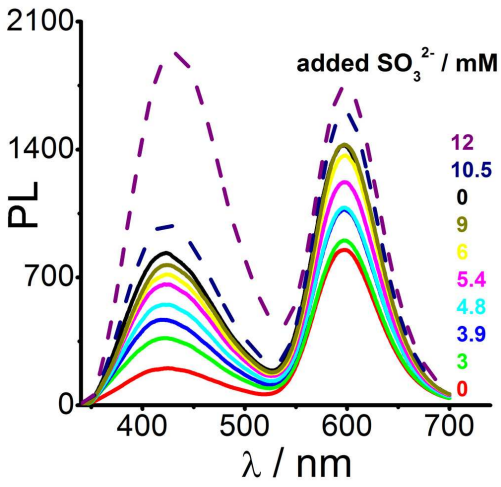

Figure S15. PL spectra of the quenched ZnS:Mn^{2+} QDs by H_2O_2 with increasing the concentrations of SO_3^{2-}. Because SO_3^{2-} can remove the surface traps by its reduction effect (Nanoscale, 2012, 4, 5954). Interestingly, the PL intensities are much stronger than that of the original QDs as excessive SO_3^{2-} is added, which well demonstrates: 1) the host and the Mn^{2+} emission quenching is attributed to the oxidation of S^{2-} and Mn^{2+}, respectively; 2) S^{6+} really exists in the original doped ZnS:Mn^{2+} QDs; 3) The host emission is more sensitive to the oxidation reaction than that of the Mn^{2+} emission.

References

1. Camara, J. N.; Suri, J. T.; Cappuccio, F. E.; Wessling, R. A.; Singaram, B. *Tetrahedron Lett.* **2002**, *43*, 1139–1141.

2. Wu, P.; Miao, L. N.; Wang, H. F.; Shao, X. G.; Yan, X. P. *Angew. Chem. Int. Ed.* **2011**, *50*, 8118–8121.

3. Zhang, M.; Liu, Y. Q.; Ye, B. C. *Analyst.* **2011**, *136*, 4558–4562.

4. Crosby, G. A.; Demas, J. N. *J. Phys. Chem.* **1971**, *75*, 991–1024.

5. Chen, H.; Kou, X.; Yang, Z.; Ni, W.; Wang, J. *Langmuir* **2008,** *24,* 5233–5237.

6. (a) Lakowicz, J. R. *Principles of Fluorescence Spectroscopy*, 2nd ed.;Kluwer Academic/Plenum Publishers: New York, 1999. (b) Medintz, I. L.; Clapp, A. R.; Mattoussi, H.; Goldman, E. R.; Fisher, B.; Mauro, J. M. *Nat. Mater.* **2003**, *2*, 630–638.